MODELING OF STATIC AND KINETIC FRICTION IN RUBBER-PAD FORMING PROCESS

by

MAZIAR RAMEZANI

Thesis submitted in fulfillment of the requirements

for the degree of

Doctor of Philosophy

November 2009

Acknowledgements

I would like to express my sincere gratitude to my supervisor, Assoc. Prof. Dr. Zaidi Mohd Ripin for his continuing encouragement, intellectual discussions and insightful suggestions. I benefited a lot from him both professionally and personally. It is an honor to be his graduate student. I would also like to thank my co-supervisor, Assoc. Prof. Dr. Roslan Ahmad for all the help.

My thanks are due to the technicians of School of Mechanical Engineering, who have helped me in my experimental works.

I would like to thank my parents for their constant support and love. They inspired and strengthened me emotionally, spiritually, and intellectually in every step of my life.

Finally, I want to thank my wife for all the support. During my research activities, her patience, understanding, encouragement and love helped me go through every obstacle and make my life here enjoyable and productive.

TABLE OF CONTENTS

LIST OF TABLES

LIST OF FIGURES

NOMENCLATURE

Roman symbols

a	contact radius, m
a'	half width of Hertzian contact, m
A_n	nominal contact area, m^2
A_r	real contact area, m^2
B	contact length, m
c	radius of the stick zone, m
d_d	distance between mean line of asperity and mean line of surface, m
E	Young's modulus, Pa
E'	equivalent modulus of elasticity, Pa
F_f	sliding friction force, N
$F_{f,c}$	friction force from asperity interaction, N
$F_{f,h}$	hydrodynamic friction force, N
F_n	normal load, N
$F_{st\max}$	maximum static friction force, N
F_t	tangential load, N
g	elasticity of the springs in SLS model, Pa
G	shear modulus, Pa
h	separation, m
h_c	lubricant film thickness, m
n	density of asperities, m^{-2}
p	pressure, Pa
P_h	maximum Hertzian pressure, Pa
P_m	mean Hertzian pressure, Pa
R'	equivalent radius, m
s	asperity height, m
t	time, s
u	sliding velocity, ms^{-1}
z	surface height, m

Greek symbols

β	mean radius of asperity, m
β_0	slope of the limiting shear stress-pressure relation, 0.047
η	dynamic viscosity at zero pressure and $40^{\circ}C$ temperature, $Pa.s$
η_0	dynamic viscosity at ambient pressure, $Pa.s$
η_d	viscosity of dashpot in SLS model, $Pa.s$
τ	shear stress, Pa
τ_L	limiting shear stress, Pa
τ_{L0}	limiting shear stress at ambient pressure, Pa
δ_n	normal approach, m
δ_t	tangential displacement, m
$\varphi(t)$	creep compliance function, Pa^{-1}
$\psi(t)$	stress relaxation function
μ	local coefficient of friction
μ_c	Coulomb coefficient of friction
μ_k	kinetic coefficient of friction
μ_s	static coefficient of friction
ρ	density, $kg.m^{-3}$
γ	scaling factor
ν	Poisson's ratio
$\theta(\bar{s})$	normalized Gaussian height distribution
σ_s	standard deviation of the asperity heights, m

Abbreviations

BL	Boundary Lubrication
EHL	Elasto-Hydrodynamic Lubrication
FEM	Finite Element Method
ML	Mixed Lubrication
SMF	Sheet Metal Forming

MODEL GESERAN STATIK DAN KINETIK DI DALAM PROSES PEMBENTUKAN BERLAPIK GETAH

ABSTRAK

Keadaan geseran di dalam simulasi proses pembentukan kepingan logam biasanyna dikira dengan menggunakan pekali geseran malar (model Coulumb). Tesis ini membangunkan model geseran statik dan kinetik berasaskan keadaan sentuhan dan mengambilkira kesan tekanan, halaju, kekasaran permukaan dan kelikatan pelincir terhadap pekali geseran. Puncak-puncak pada permukaan dimodel secara statistik dengan taburan Gauss dan puncak-puncak pada permukaan getah dianggap sebagai elastik-likat. Pada permukaan bersentuh di antara acuan dan kepingan logam jumlah daya di dalam arah normal di anggap di kongsi bersama oleh daya angkatan hidrodinamik dan daya-daya saling tindak puncak-puncak pada permukaan. Model geseran yang dibangunkan menunjukkan pada daya normal yang rendah, pekali geseran mengurang dengan banyak apabila beban meningkat dan mencapai tahap malar pada beban tinggi. Pekali geseran kinetik mengurang dengan pertambahan halaju gelinciran dan daya arah normal. Secara teorinya dapat ditunjukkan pekali geseran menjadi lebih besar bagi permukaan yang lebih kasar dan dengan pelincir yang lebih likat, pekali geseran kinetik berkurangan. Sebagai tambahan ujikaji dan simulasi pembentukan berlapik getah dilakukan. Lengkuk gesearan daripada pengiraan menggunakan model geseran yang baru dilaksanakan di dalam kod unsur terhingga ABAQUS/Standard. Keputusan simulasi menunjukkan model geseran yang baru memberikan korrelasi yang lebih baik dengan keputusan ujikaji berbanding menggunakan model Coulumb dari segi lengkuk beban hentam-lejang dan ramalan penipisan. Ralat bagi ramalan kaedah unsur terhingga ialah 8% bagi model geseran Coulumb dan 5.6% bagi model geseran kinetik. Ralat ini berkurangan kepada 4.8% bila model geseran statik digunakan.

MODELING OF STATIC AND KINETIC FRICTION IN RUBBER-PAD FORMING PROCESS

ABSTRACT

The frictional behaviour in sheet metal forming simulations is often taken into account by using a constant coefficient of friction (Coulomb model). This thesis develops static and kinetic friction models which are based on local contact conditions and consider the effect of pressure, velocity, surface roughness and lubricant viscosity on coefficient of friction. The surface asperities were modeled using statistical Gaussian distribution and the behavior of rubber asperities was assumed to be viscoelastic. In lubricated contact surface between die and sheet, the total normal load was assumed to share by the hydrodynamic lifting force and the asperity interacting force. According to developed friction models, at low normal loads the static friction coefficient decreases sharply with increasing normal load and reaches a quite stable level at higher loads. The coefficient of kinetic friction decreases with increasing the sliding velocity and normal load. It was shown theoretically that the coefficient of friction is larger for rougher surfaces, and by increasing the lubricant viscosity, the coefficient of kinetic friction decreases. Furthermore, rubber-pad forming experiments and simulations were performed. The calculated friction curves using the new friction models were implemented in the finite element code ABAQUS/Standard. From the results of simulations it was found that the new friction models have better correlation with experimental results compared to traditional Coulomb friction model, in terms of punch load-stroke curve and thinning prediction. The FE prediction error for maximum punch load is 8% using Coulomb friction model and 5.6% using the kinetic friction model. The error decreases to 4.8% using the static friction model.

Chapter 1

Introduction

1.1 Rubber-pad forming process

All Sheet Metal Forming (SMF) processes have in common that they are mostly performed with the aid of presses which drive the tools to deform the initially flat sheet material into a product. The sliding of a plastically deforming sheet against the tools makes both tribological as well as mechanical knowledge necessary for optimum processing.

The conventional SMF process is performed through a rigid punch, which together with a blank-holder, forces the sheet metal to slide into a die and comply with the shape of the die itself. Rubber forming adopts a rubber pad contained in a rigid box in which one of the tools (die or punch) is replaced by the rubber pad. The elastomer incompressibility is exploited: deforming at constant volume, it exerts a hydrostatic pressure on the sheet metal. Such a technology possesses several advantages: in this process, only a single rigid tool half is required to form a part. One rubber pad takes the place of many different die shapes, returning to its original shape when the pressure is released. Tools can be made of low cost, easy-to-machine materials due to the hydrostatic pressure exerted on the tools. The bending radii changes progressively during forming process. Using rubber as flexible punch, thinning of the workpiece, as occurs in conventional deep drawing, is reduced considerably. The same tool set-up can be used to stamp different materials and different thicknesses. Components with excellent surface finish can be formed as no tool marks are created. The set-up time is reduced, because the punch-to-die alignment procedure is

no longer necessary. Lubrication is usually not needed. Disadvantages consist of the short operating life of the rubber pads, lower stamping pressure which results in parts with less sharpness that may require subsequent hand works and the production rate is low. Rubber forming technology is particularly suited to the production of prototypes and small series (Thiruvarudchelvan, 1993 and Sala, 2001).

Rubber forming can be divided into three main categories: i.e., rubber-pad forming, fluid-cell forming and fluid forming. Among these techniques, rubber-pad forming process (see, Figure 1.1) is the oldest and simplest, its advantages consisting of tooling profitability and production flexibility, suited for small series. The rubber pads in this method may be constructed either solidly or laminated. The laminated pad comprised of sheets of rubber placed over one another. The advantage they have is that the working surface can be restored by turning the top layer over or replacing it. The rubber chamber and form block are made of steel or cast iron (able to sustain forming pressures of 50-140 *MPa*) and the rubber pad is made of a soft (50-75 Shore hardness) elastomer. Maximum stamping depth seldom exceeds 50 *mm*, which can be increased by using thicker pads and more powerful presses (Sala, 2001).

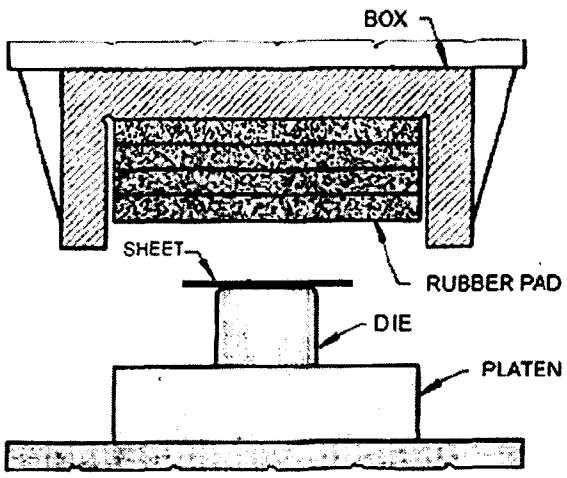

Figure 1.1 Rubber-pad forming process (Sala, 2001).

The methods belonging to fluid-cell forming category (see, e.g., Figure 1.2) use the elastomer as a medium placed between sheet metal and a flexible container (fluid cell) filled with a hydraulic fluid and able to apply a hydrostatic pressure to the workpiece. These methods can produce deep (up to 400-450 *mm*), undercut and intricate components. In the fluid-cell forming method shown in Figure 1.2, a pump pressurizes a flexible fluid cell. The fluid cell wall is protected from the contact with sheet metal by a soft rubber pad. Without punch movements, the fluid cell expansion forces the rubber pad to comply to the die contour, thus exerting a hydrostatic pressure on the sheet metal to take the shape of the die (Sala, 2001).

Fluid forming (or rubber-diaphragm forming) technologies (see, e.g., Figure 1.3) also exploit flexible punch to prevent stress concentrations, they differ from rubber-pad and fluid-cell forming processes because the forming pressure depends on the forming depth. In the fluid forming method shown in Figure 1.3, a hydraulic fluid, pressurized by an actuator forces the sheet metal against the die contour, while an inlet valve removes trapped air; a rubber diaphragm shields the sheet metal and distributes pressure.

Compared to fluid-cell forming and rubber-diaphragm forming, rubber-pad forming has a further advantage that sealing problems and the possibility of leakage of the high-pressure liquid are eliminated (Thiruvarudchelvan, 2002). Up to 60% of all sheet metal parts in aircraft industry such as frames, seat parts, ribs, windows and doors are fabricated using rubber-pad forming processes (Lascoe, 1988). In other industries, for instance automotive industry, this process is mainly used for prototypes or pilot productions. In this thesis, rubber-pad forming process is adopted for analysis and experiments, because both static and kinetic friction regimes are available simultaneously during this process.

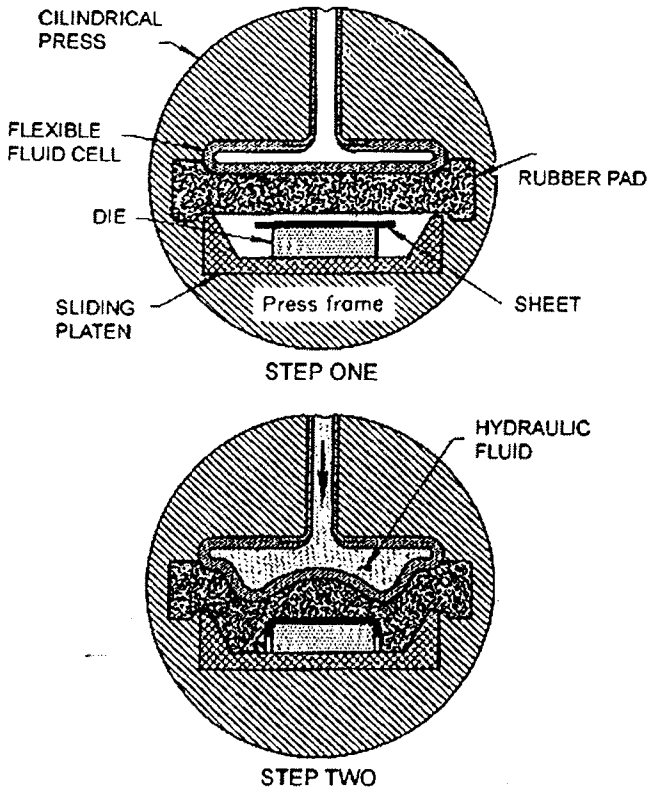

Figure 1.2 Fluid-cell forming process (Sala, 2001).

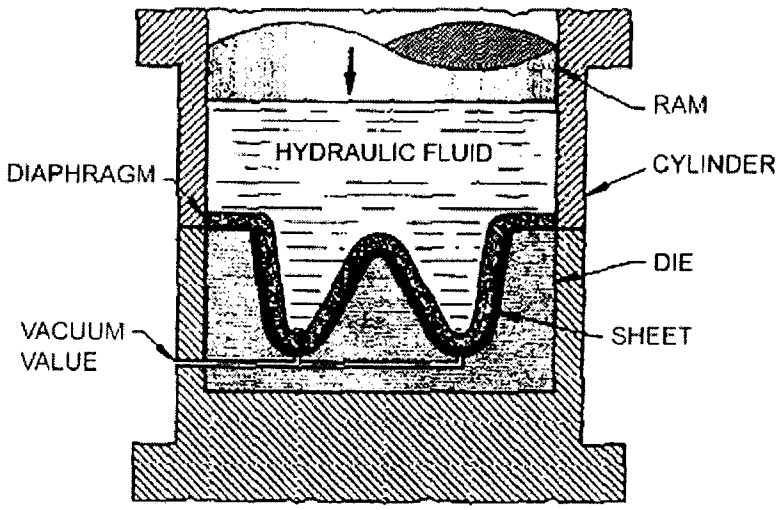

Figure 1.3 Fluid (rubber-diaphragm) forming process (Sala, 2001).

1.2 Friction in rubber-pad forming process

"Tribology" is the science and technology of interacting surfaces in relative motion. It is best studied by looking at the system of parameters influencing the frictional behaviour of bodies in contact with each other. This means that not only the contact itself is of importance but also that the environment of the contact plays a role. A general tribo-system is shown in Figure 1.4. This system consists of the following elements: two bodies which interact with each other, a lubricant and the environment.

In recent years, the finite element method (FEM) has been widely used to simulate SMF operations. The simulations are used for quality control and problem analysis such as tearing, wrinkling and surface distortion. The usefulness of such analysis is limited by the accuracy of the description of the friction phenomena in the sheet/tool contact area (Lee et al., 2002). For SMF processes, the frictional behaviour depends on several parameters such as the contact pressure, sliding speed, sheet and tool material, surface roughness, lubricant and concurrent deformation (Wilson, 1979). Especially when the blank thickness/blank area ratio is small, the friction influences the material flow and with this the final strain distribution. Since all of these variables influence friction, the question arises as whether the Coulomb simple friction model is capable of describing the real frictional properties of sheet metal forming processes. Some results have pointed out that a friction model based on local contact conditions is more advantageous than the Coulomb friction model, especially in a range of higher sliding velocities (see, e.g., Matuszak, 2000).

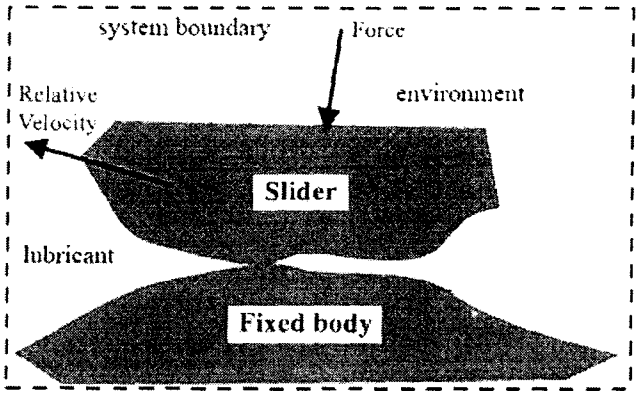

Figure 1.4 Representation of a tribo-system.

There are two kinds of friction in rubber-pad forming process: static friction between sheet blank and rubber and kinetic friction between sheet blank and die. It is well known that the static coefficient of friction is generally larger than the kinetic one when a tangential force is applied to a slider.

1.2.1 Static friction

In practice static friction is usually associated to the "stick" of surfaces in contact, i.e., the pre-sliding friction. It is well known from everyday experience that to displace one body relative to another when the bodies are subjected to a compressive force necessitates the application of a specific tangential force, known as the static friction force, and until the required force is applied the bodies remain at rest. Accurate prediction of the static friction force may have an enormous impact on a wide range of applications such as rubber-pad forming process, bolted joint members, workpiece-fixture element pairs, static seals, clutches, compliant electrical connectors, magnetic hard disks and MEMS devices, to name just a few (Kogut and Etsion, 2004).

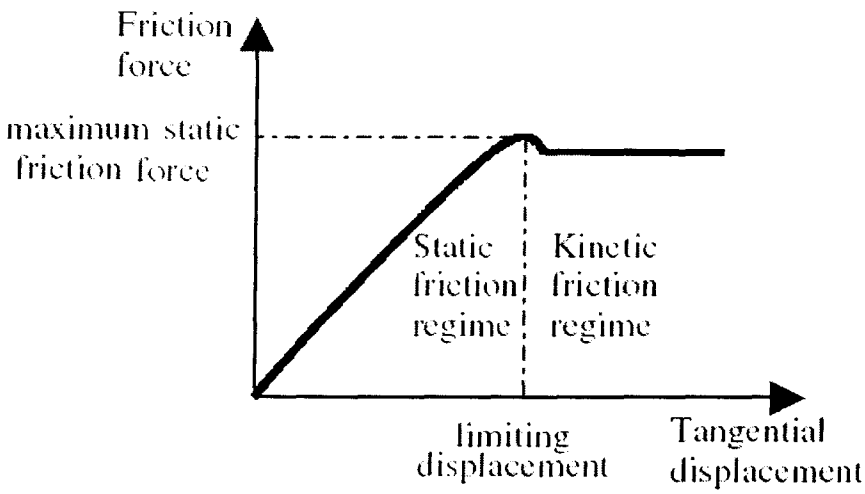

Figure 1.5 The relation between friction force and tangential displacement.

In the static friction regime, the friction force increases with increasing tangential displacement up to the value necessary to initiate macro-sliding of the bodies in contact, as depicted in Figure 1.5. Although, the bodies are macroscopically in rest, a micro-displacement occurs at the interface which precedes the macro-sliding situation (Persson et al., 2003). This micro-displacement can reach relatively large values when one of the surfaces in contact has a low tangential stiffness compared to the other surface, as for instance in the rubber/metal contact (Deladi et al., 2007). The main characteristic parameters of the static friction regime are the maximum static friction force at which macro-sliding initiates and the corresponding micro-displacement. This maximum force is given by the peak seen in Figure 1.5. A comprehensive analysis of the mechanisms and parameters involved in this preliminary stage of friction is presented in Chapter 4. Once the bodies are set in motion, a certain force is required to sustain it. This is the kinetic friction force which will be discussed in the next section.

1.2.2 Kinetic friction

As depicted in Figure 1.4, most of the tribo-systems consist of two or more interacting bodies and a lubricant. In the case of metal/tool tribo-systems in metal forming processes a liquid lubricant is often applied; animal fats and natural oils were used in the past. Application of lubricants can have several reasons:

- Lowering the total force needed for the operation, usually the friction force for lubricated contacts is much lower than for dry contacts.
- Prevention of wear of the metal and the tools, caused by adhesion and adhesion related problems.
- Assurance that the products will meet the quality requirements. It is possible to control the material flow into the die by means of friction and lubrication (Schey, 1983).

Often, the friction force in a lubricated tribo-system is described as a function of one or more of the operational parameters. Depending on the value of the parameter(s) used, a tribo-system can operate in the following lubrication regimes:

- *(Elasto) Hydrodynamic Lubrication ((E)HL) regime:* there is no physical contact between the interacting surfaces of the contact, the load is carried completely by the lubricant film between the surfaces. The coefficient of friction, μ, therefore has a rather low value, of the order of 0.01.
- *Boundary Lubrication (BL) regime:* there is physical contact between the interacting surfaces, the load is carried entirely by the surface roughness peaks which are in physical contact with each other. Friction is determined by the layers adhered to the surfaces.

■ *Mixed Lubrication (ML) regime:* this is the regime in-between the BL-regime and the (E)HL-regime, the load on the contact is partly carried by the lubricant and partly by the interacting surface roughness peaks.

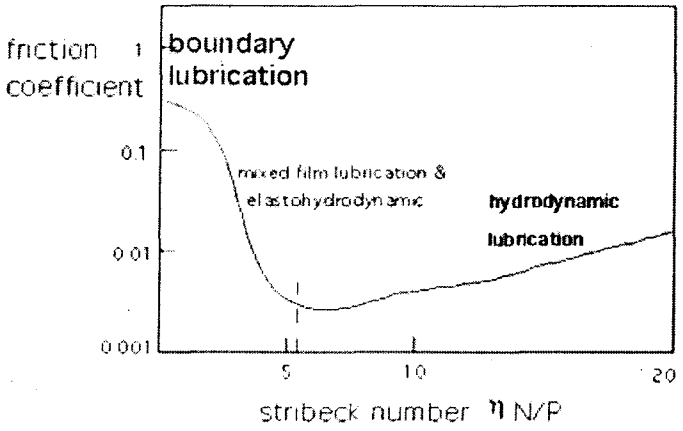

Figure 1.6 Sample generalized Stribeck curve.

As cited by Jacobson (2003), in the beginning of last century, Stribeck (1902) was the first who reported the dependence of the coefficient of friction on the shaft velocity in journal bearings. He presented μ vs. shaft velocity curves which show the three described lubrication regimes referred to as Stribeck curves. Most lubricated tribo-systems show Stribeck-type frictional behavior. This seems also the case for metal/die contacts under metal forming conditions which is because of the lubrication generally applies to metal/die interface and roughness of sheet and die. In Figure 1.6, a generalized Stribeck curve is shown. In this figure, the three lubrication regimes can be distinguished. The boundary regime is situated on the left-hand part of the curve. The right-hand part of the curve shows a relatively low coefficient of friction, this is the (elasto) hydrodynamic regime. In between these two regimes, the mixed regime can be found, this is the part of the curve in which the coefficient of

friction depends strongly on the Stribeck number $\frac{\eta.N}{P}$, where η is dynamic lubricant viscosity, N is the rotational velocity and P is the mean contact pressure.

1.3 Objectives

The main objectives of this research are:

(1) Development of FE model for rubber-pad forming process and the study of process parameters such as rubber material, stamping velocity, rubber-pad thickness and coefficient of friction.

(2) Developing static and kinetic friction models based on local contact conditions such as normal pressure, surface characteristics, lubricant viscosity and sliding velocity which are suitable for rubber-pad forming process to overcome the problem of accuracy of sheet metal forming simulations, and

(3) Verification of new friction models integrated in FE models with experimental data.

1.4 Overview

A review of the available literature will be presented in Chapter 2. The finite element simulation and experimental procedure of quasi-static rubber-pad forming process will be explained in Chapter 3. Some key process parameters such as rubber material, stamping velocity, rubber-pad thickness and friction conditions are investigated in details. Non-linear finite element analysis using commercial software ABAQUS/Standard is conducted to analyze stress and strain distribution and deformation mechanisms during an axisymmetric rubber-pad forming process. Chapter 4 deals with theoretical modeling of static friction in rubber/metal contact

and kinetic friction in metal/metal contact which happens between rubber/workpiece and die/workpiece in rubber-pad forming process. The friction models which developed extensively in Chapter 4 will be implemented to rubber-pad forming simulation to investigate its efficacy and the results will be presented in Chapter 5. The results of proposed friction models will be compared with traditional Coulomb friction model. Chapter 6 lists the conclusions and future work for the different studies undertaken. The motivation for those studies, the method used in them and the new insights gained from them are summarized.

Chapter 2

Literature review

2.1 Introduction

In this chapter, the review of available literature is presented. It starts with rubber-pad forming process and follows with the works performed on contact mechanics and static and kinetic friction modeling. A brief discussion is presented at the end of the chapter.

2.2 Rubber-pad forming process

Several studies have been carried out to analyze rubber-pad forming process. Browne and Battikha (1995) presented an experimental study of the rubber-pad forming process to investigate the capability of the process and to optimize the process parameters. They analyzed the use of different types of lubricants at the blank and its interfaces. The dependence of the clamping force for the prevention of wrinkling and cracking on the type of blank material was also investigated.

Thiruvarudchelvan (2002) and Thiruvarudchelvan and Tan (2005) introduced several techniques for the use of flexible tools in metal forming. They presented the principles involved in friction-aided sheet metal forming techniques, the design of the flexible tools, the actual prototype devices fabricated and tested, and the experimental data from forming operations.

Sala (2001) optimized the rubber-pad forming process of an aluminum alloy fuselage frame belonging to AerMacchi MB-339 trainer aircraft using a specific finite element code. Several effects, depending on stamping velocity, component geometry, sheet metal heat treatment, elastomeric rubber-pad constitutive law and

thickness were taken into account. It was shown by his work that how the preliminary tuning of these parameters lead to minimizing defects, increasing component quality and reducing set-up times.

Dirikolu and Akdemir (2004) carried out a 3D finite element simulation study concerning the flexible forming process to investigate the influence of rubber hardness and blank material type on stress distribution in the formed blank. Their investigations showed the effectiveness of finite element simulations in process design and exposed the rubber hardness, blank material type, contact friction and die design as crucial parameters that require adjustment before actual operations.

Peng et al. (2009) investigated the sheet soft punch stamping process to fabricate micro channels via numerical simulations and experiments. Grain size of sheet metal, hardness of soft punch and lubricant condition, were studied in details and the numerical results were partially validated by experiments. They found that sheet metal with small grain size is prone to obtain high formability. Larger friction coefficient (up to 0.3) between the sheet and the rigid die may make the sheet thinning quickly which decreases the formability, while the friction between the sheet metal and the soft punch does not play an important role. They also reported that the hardness of soft punch is not a decisive parameter to the final quality of the workpiece.

2.3 Asperity contact models

When two solids are squeezed together they will in general not make atomic contact everywhere within the apparent contact area and contact happens only on peak asperities of surfaces. Tabor (1981) reviewed the state of understanding of friction phenomenon as it existed three decades ago. Friction was originally thought

to be due to the resistance of asperities on one surface riding over the asperities of the mating surface. The distinction between static and kinetic friction was attributed to the asperities jumping over the gap between neighboring asperities on the other surface during sliding.

Surface contact modeling is an essential part of any friction model (Adams et al., 2003). It consists of two related steps. First, the equations representing the contact of a single pair of asperities are determined. Second, the cumulative effects of individual asperities are determined. Conventional multi-asperity contact models may be categorized as predominately uncoupled or predominately coupled. Uncoupled contact models represent surface roughness as a set of asperities, often with statistically distributed parameters. The effect of each individual asperity is local and considered separately from the other asperities; the cumulative effect is the summation of the actions of individual asperities. Coupled models include the effect of the loading on one asperity on the deformation of neighboring asperities. Such models are far more complex mathematically than the uncoupled models and for that reason have been used less frequently.

Hertz in 1882, presented the solution for the single asperity contact area between two elastic bodies. The assumptions of Hertz contact problem are: (1) the contact area is elliptical; (2) Each body is approximated by an elastic asperity loaded over an elliptical contact area; (3) the dimensions of the contact area are small compared to the dimensions of each body and to the radius of curvature of the surfaces; (4) the strains are sufficiently small for linear elasticity to be valid; and (5) the contact is frictionless and only a normal pressure is transmitted. In Hertz contact theory, area of contact, contact radius and maximum contact pressure are given by simple equations

which depend upon the Young's moduli, the Poisson's ratios, the radius of curvature, and the applied force (Carbone and Bottiglione, 2008).

In a pioneering study, Archard (1957) showed that in a more realistic model of rough surfaces, where the roughness was described by a hierarchical model consisting of small spherical bumps on top of larger spherical bumps and so on, the area of real contact is proportional to the load. This model explains the basic physics in a clear manner, but it cannot be used in practical calculations because real surfaces cannot be represented by the idealized surface roughness assumed by Archard. A somewhat more useful model, from the point of view of applications, was presented by Greenwood and Williamson (1966). The Greenwood and Williamson model assumes that in the contact between one rough and one smooth surface: (1) the rough surface is isotropic; (2) asperities are spherical near their summits; (3) all asperity summits have the same radius of curvature while their heights vary randomly with a Gaussian distribution; (4) there is no interaction between neighboring asperities; and (5) there is no bulk deformation. This model predicts that the area of real contact is nearly proportional to the load. A more refined model based on the same picture was developed by Bush et al. (1975). They approximated the asperities with paraboloids to which they applied the Hertzian contact theory. The height distribution was described by a random process, and they found that at low squeezing force the area of real contact increases linearly with normal force. Several other contact theories are reviewed in Carbone and Bottiglione (2008) and Persson (2006).

2.4 Static friction in rubber/metal contact

Static friction, defined as the tangential force required to initiate relative motion of two contacting bodies, is associated with many important mechanical devices and

machines. A great amount of research work has been done in measuring and modeling static friction. The elastic-plastic spherical contact under combined normal and tangential loading is a classical problem in contact mechanics which is applicable in modeling of friction between rough surfaces. The treatment of combined normal and tangential loading of elastic spherical contact stems from the classical work of Mindlin (1949). According to the Mindlin model, the contact area between two spheres under combined loading consists of a central stick region surrounded by an annular slip zone. As the tangential load increases, the central stick region gradually diminishes and finally disappears. At this moment full sliding begins which satisfies the Coulomb friction law, that is, the tangential load equals the product of the normal load and a predefined static friction coefficient. The normal loading in this work is assumed frictionless, and the contact area and pressure distribution follow the Hertz solution even when the tangential load is applied. Chang, Etsion and Bogy (1988) presented a model (CEB friction model) for predicting the static friction coefficient of rough metallic surfaces. The CEB friction model uses a statistical representation of surface roughness following a Gaussian distribution and calculates the static friction force that is required to fail all of the contacting asperities, taking into account their normal preloading. In CEB model, the mechanism involves plastic flow of pre-stressed asperities. Related to the temperature, possible static friction mechanisms are the asperity creep at lower temperatures and welding of asperities at higher temperatures.

Rubber/metal contact is found in a large variety of applications, such as rubber-pad forming processes, vibration control applications, power transmission systems and seals. There are many papers in the literature about rubber friction regarding kinetic friction (see, e.g., Persson et al., 2003), but only a few concerning static friction. The

static friction force was investigated by Roberts and Thomas (1976) for smooth rubber hemispheres in contact with glass plates. Their experiments carried out on soft rubber suggest that the magnitude of the static friction force is related to the elastic deformation of rubber prior to the appearance of the elastic instabilities.

The preliminary stage of friction was studied experimentally by Barquins (1993) in rubber/glass contact. The evolution of the contact area was recorded by means of a camera mounted on an optical microscope. Superimposing the frames has shown a contact area which comprises a central adhesive zone, surrounded by an annulus of slip. Friction forces were measured with the help of an elastic system and displacement transducers.

The experiments of Adachi et al. (2004) carried out on rubber balls in contact with glass plates revealed also the process of partial slip and its propagation with increasing tangential load as described theoretically by Mindlin (1949).

Deladi et al. (2007) developed a static friction model for rubber/metal contact that takes into account the viscoelastic behaviour of rubber. This model is based on the contact of a viscoelastic/rigid asperity couple. Single asperity contact was modeled in such a way that the asperities stick together in a central region and slip over an annulus at the edge of the contact. The slip area increases with increasing tangential load. Consequently, the static friction force is the force when the slip area is equal to the contact area. Using the model, the traction distributions, contact area, tangential and normal displacement of two contacting asperities were calculated. The single asperity model was then extended to multi-asperity contact, suitable for rough surfaces.

2.5 Kinetic friction in metal/metal contact

From the early experimental work of Amontons in 1699, it was observed that friction is directly proportional to the applied load and independent of the surface nominal contact area. Coulomb in 1785, completed Amontons work with the third law that kinetic friction force is independent of sliding velocity. These early observations gave rise to the classic laws of friction, which resulted in a proportionality constant, known as the friction coefficient. However, today it is well recognized that friction coefficient values depend on many other conditions besides the contacting material pairs, such as surface roughness, lubricant viscosity, surface energy, contact load and temperature.

The development of kinetic friction models for SMF simulations is complicated by the fact that any of a variety of lubrication regimes may co-exist in the sheet/tooling interface. Wilson (1979) described four basic lubrication regimes in metal working: thick film, thin film, mixed and boundary lubrication regimes. Moreover, he showed that the traditional Coulomb friction model is inappropriate for sheet metal forming simulations, because it does not predict the lubrication regimes. Schey (1983) provided a review of many different ways of measuring or inferring friction in metal forming operations. One of the most useful methods is that of Schey (1996) who explored the effect of drawing speed and lubricant viscosity on coefficient of friction using drawbead simulation tests. The results showed that the coefficient of friction decreases with increasing the viscosity × velocity product. Saha et al. (1996) investigated the relationship between friction and process variables including sliding speed, strip strain and strain rate in the boundary lubrication regime using a sheet metal forming simulator which stretches a strip around a cylindrical pin. Friction was found to decrease with increasing sliding velocity for all test conditions.

Stribeck (1902) is credited for carrying out the first systematic experiments unfolding a clear view of the characteristic curve of the coefficient of kinetic friction versus speed. In recognition of his contribution, this curve is called the "Stribeck curve" (Jacobson, 2003). Works on the Stribeck curve fall into two categories: one is the experimental examination of its variation by altering the material property, the surface finish, the viscosity of the oil, and the operating conditions; the other is theoretical exploration of its behavior that parallels the development of the modeling of mixed lubrication.

In Gelinck and Schipper (2000), a model is presented in order to predict the Stribeck curves for line contacts. This model is based on the combination of the Greenwood and Williamson (1966) contact model and the full film theory using the mixed lubrication model of Johnson et al. (1972). With this model, one is able to predict friction and determine the transitions between the different lubrication regimes: elasto-hydrodynamic lubrication (EHL), mixed lubrication (ML), and boundary lubrication (BL) regimes. This model is based on the assumption that enough lubricant is supplied to the contact, e.g., fully flooded conditions.

Faraon and Schipper (2007) developed a mixed lubrication model in order to predict the Stribeck curves for starved lubricated line contact. This model is based on a combination of the contact model of Greenwood and Williamson (1966) and the elasto-hydrodynamic (EHL) film thickness for starved line contacts.

In the work of Wolveridge et al. (1971), a correction on the film thickness formula for line contacts due to starvation is presented. Combining this modified film thickness relation for starved line contacts with the model of Gelinck and Schipper (2000) will result in a mixed lubrication model for starved lubricated line contacts.

Lu et al. (2006) presented the Stribeck curves of a series of experiments under various oil inlet temperatures and loads and verified the curves with a theoretical model. This model is based on the Bair and Winer model (1979) to describe the shear stress of the lubricant. Their theoretical analysis provided a simple, but realistic model, for prediction of Stribeck curves.

2.6 Conclusion

The various literature reviewed in this chapter has shown that to date, the models of friction which take into account the various local contact conditions such as velocity, pressure, lubricant viscosity, roughness and temperature are available and have been well researched. The published work to date only used Coulomb friction model in the rubber-pad forming simulations. The application of such static and kinetic friction models on rubber-pad forming simulations have not been reported anywhere. The existence of various lubrication regimes in metal working would suggest that Coulomb friction model is inadequate for application in SMF simulations. It necessitates the application of new friction models in SMF simulations to ensure the accuracy and efficiency of finite element simulations and therefore the static and kinetic friction models suitable for rubber-pad forming process are studied in this thesis.

Chapter 3

Static and kinetic friction models for rubber-pad forming

3.1 Introduction

When a metal forming process is observed, it is clear that the conditions in all the different contacts are very different. For most forming simulations the value of coefficient of friction is taken as a constant, neglecting the fact that friction depends on a large number of parameters, e.g., the micro-geometry, the macro-geometry, the lubricant and the operational parameters: velocity, temperature and normal load. If one of the parameters changes, the coefficient of friction will also change (Matuszak, 2000). Often, several metal forming simulations with different values for the coefficient of friction have to be performed before the simulation provides acceptable results. It is clear that these simulations have no predicting power at all (Lee et al., 2002) and friction models based on local contact conditions are needed.

In this chapter, at first a single-asperity static friction model is presented and subsequently, a multi-asperity static friction model between viscoelastic asperities and a rigid flat under combined normal and tangential loading condition is developed for rubber-pad/metal sheet contact taking into account the viscoelastic behaviour of rubber and local contact conditions. Subsequently, a kinetic friction model is developed for die/metal sheet contact based on Stribeck frictional behavior.

3.2 Coulomb friction model

The easiest and probably the most well known friction model is Coulomb friction model. Though it greatly over simplifies the frictional phenomena it is widely used to

describe the friction in mechanical contacts. In this model, the ratio between friction force and normal force, defined as the coefficient of friction, is considered to be constant. Coulomb friction model can be formulated as

$$F_f = \mu_c F_n \tag{3.1}$$

where μ_c is the Coulomb coefficient of friction, F_f is the sliding friction force and F_n the normal load in the contact.

3.3 Single-asperity static friction model for rubber/metal contact

The contact between surfaces is composed of many asperity couples that carry the load. The first step in modeling two surfaces in contact is based on the determination of the contact parameters between a pair of asperities (Deladi et al., 2007). When two elastic spherical asperities are loaded by a normal force F_n, the radius of the contact circle, the pressure and the normal approach are given by Hertz theory. If, subsequently, a tangential force F_t is applied, the shear stress within the contact and the tangential displacement of bodies are specified by Mindlin theory. According to Mindlin (1949), the resulting infinite tangential traction at the edge of the contact is released by micro-slip and the contact area comprises a stick region surrounded by an annulus of slip (see, Figure 3.1). This micro-slip can be calculated using the solution proposed by Johnson (1985).

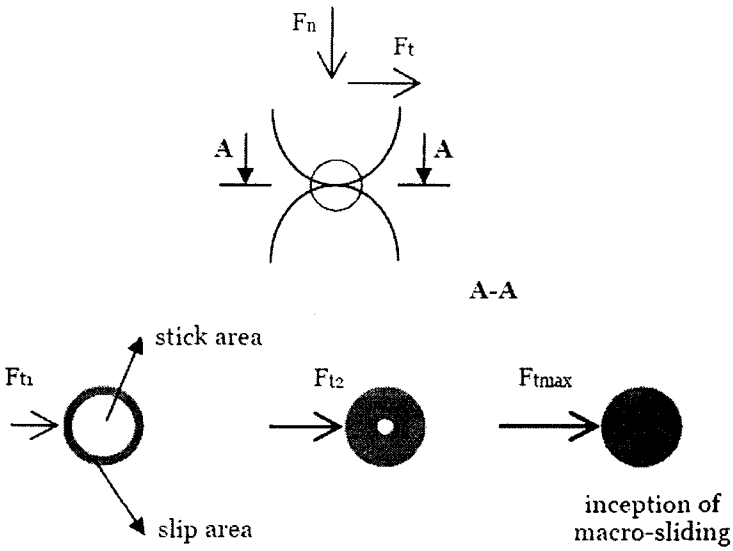

Figure 3.1 Evolution of the contact area (top view) according to Mindlin theory (Mindlin, 1949).

Rubber materials exhibit both elasticity and viscous resistance to deformation. The materials can retain the recoverable (elastic) strain energy partially, but they also dissipate energy if the deformation is maintained. Viscoelasticity is the property of materials that exhibit both viscous and elastic characteristics when undergoing deformation. Viscous materials resist shear flow and strain linearly with time when a stress is applied. Elastic materials strain instantaneously when stretched and just as quickly return to their original state once the stress is removed. Viscoelastic materials behaviour can be modeled using springs and dashpots connected in series and/or in parallel. A dashpot is connected in parallel with a spring in Figure 3.2(a). This is known as a Voigt element. If deformed, the force in the spring is assumed to be proportional to the elongation of the assembly, and the force in the dashpot is assumed to be proportional to the rate of elongation of the assembly. With no force acting upon it, the assembly will return to its reference state that is dictated by the

rest length of the spring. In this model, if a sudden tensile force is applied, some of the work performed in the assembly is dissipated in the dashpot while the remainder is stored in the spring. The applied force is analogous to the deforming stress and the elongation is analogous to the resulting strain. The viscous resistance to deformation represented by the dashpot introduces time dependency to the response of the assembly where this dependency is dictated by the spring and dashpot constants.

A dashpot is connected in series with a spring is shown in Figure 3.2(b). This is called a Maxwell element. In this assembly, if a sudden tensile force is applied, it is the same in both the spring and the dashpot. The total displacement experienced by the element is the sum of the displacements of the spring and the dashpot. The response of rubber to changes in stress or strain is actually a combination of elements of both mechanical models (see, Figure 3.2(c)). The response is always time-dependent and involves both the elastic storage of energy and viscous loss.

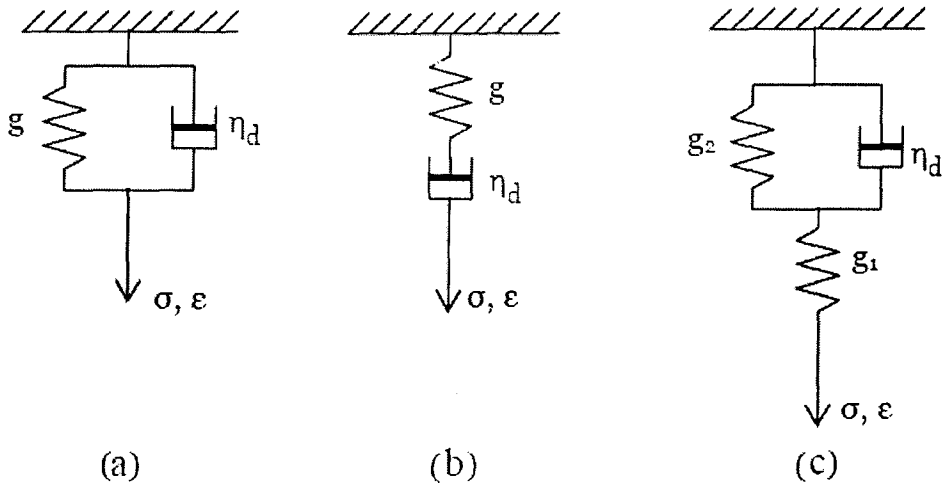

Figure 3.2 Mechanical models representing the response of viscoelastic materials: (a) Voigt model, (b) Maxwell model, (c) SLS model.

The Standard Linear Solid (SLS) model gives a relatively good description of both stress relaxation and creep behavior. Stress relaxation is the time-dependent decrease